N88-14554

METEOR DETECTION ON ST (MST) RADARS

S. K. Avery

University of Colorado
Boulder, Colorado

The ability to detect radar echoes from backscatter due to turbulent irregularities of the radio refractive index in the clear atmosphere has lead to an increasing number of established mesosphere - stratosphere - troposphere (MST or ST) radars. Humidity and temperature variations are responsible for the echo in the troposphere and statosphere and turbulence acting on electron density gradients provides the echo in the mesosphere. The MST radar and its smaller version, the ST radar, are pulsed Doppler radars operating in the VHF - UHF frequency range. They provide nearly continuous wind measurements in real time in the troposphere and lower stratosphere and during daylight hours in the mesosphere. Several new radars have been proposed including a network in the United States that will replace the national rawinsonde network for operational use. The majority of the new radars will be the smaller ST radar which probes only the troposphere and lower stratosphere. The ST radar is much less expensive than the more powerful MST radars ($150,000 vs $1,500,000, excluding labor, real estate, and operations and maintenance). For those people interested in upper atmosphere dynamics, the ST radar is not a very useful tool due to the limited height of usable echo returns. However, the presence of strong meteor echoes in the upper mesophere has been noted on ST radars (AVERY et al., 1983). These echoes can be used to determine upper atmosphere winds at little extra cost to the ST radar configuration. In addition, the meteor echoes can supplement mesospheric data from an MST radar. In this paper I will describe the detection techniques required on the ST radar for delineating meteor echo returns.

A basic radar schematic for the ST/MST radar is shown in Figure 1. The radar is very similar to the more traditional meteor radars and the major differences between the two systems are the antenna configuration and the echo detection and processing of the data. Narrow antenna beamwidths are required in an ST/MST radar. Consequently these systems use large antenna arrays and are generally more expensive. Coherent detection of the received signal from three antenna beam directions gives a measure of the complete wind field. Coherent integration and FFT techniques are used to determine the Doppler frequency which gives a measure of the radial velocity. Temporal resolution is approximately one minute with a possible height resolution of 150 m.

Meteor echoes observed with a ST/MST radar have a well defined location due to the narrow beam width of the ST/MST radar as compared with the wide beams of the more traditional meteor radars. The problem with using meteor echo returns, either on a meteor radar or a ST/MST radar is in finding the Doppler frequency using a fairly short time series. Pulse pair processing is usually done to determine the Doppler frequency (STRAUCH et al., 1978). Due to the narrow beamwidth and antenna pointing directions meteor echo rates are lower on the ST/MST radar than a meteor radar. However, there are a sufficient number of echoes to determine the winds and tidal harmonics of the wind over time intervals greater than a week.

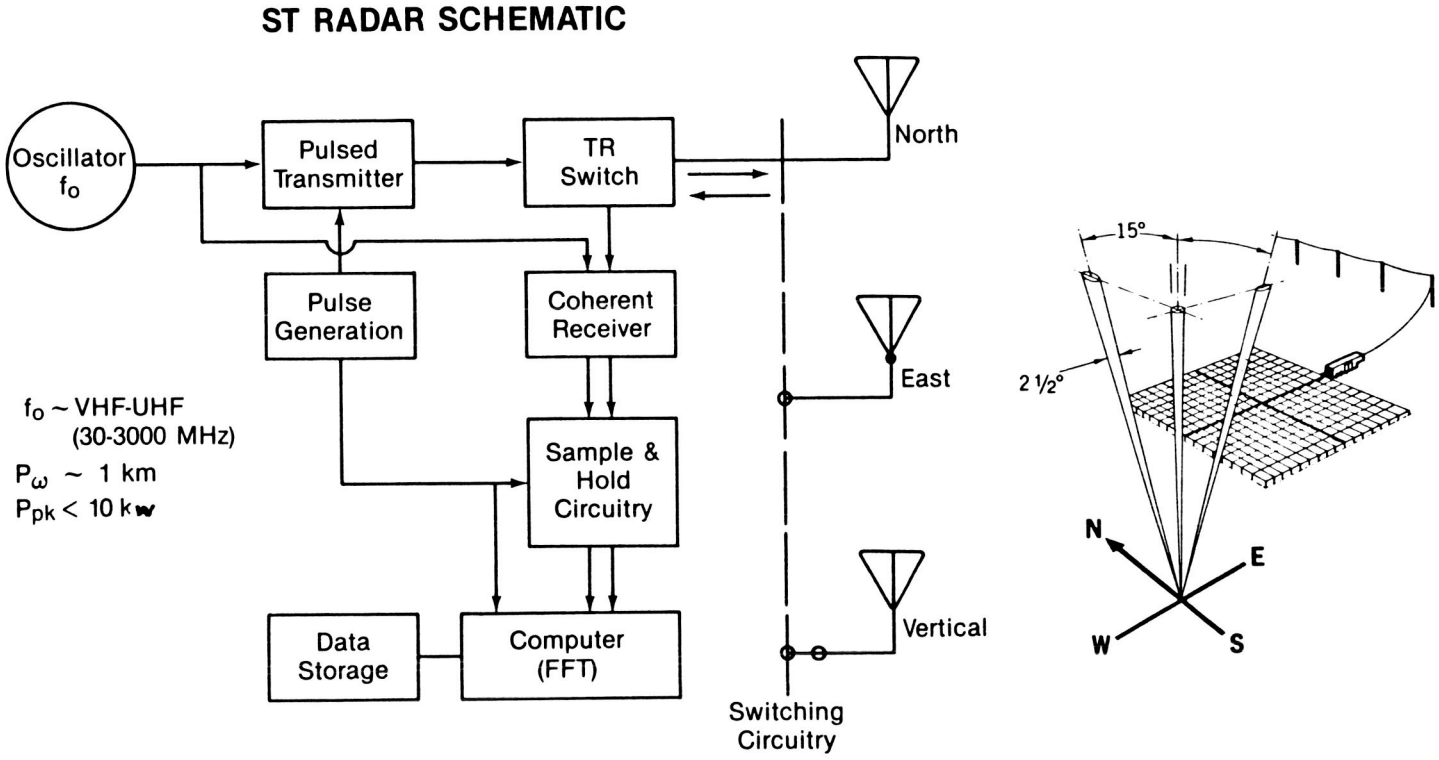

Fig. 1 Basic ST/MST radar schematic.

The existence of meteor echo returns is shown in the backscattered power profiles shown in Figure 2. These plots are from a recent experiment we performed using the Jicamarca Radio Observatory in Peru which is designed primarily for ionsopheric research. The top plot shows a well defined meteor echo at 83 km. The presence of the echo is clearly seen in the power spike on the two-dimensional plot. The three dimensional plot shows the height and temporal evolution of the meteor echo. The echo lasted for 10 pulses which corresponds to a time interval of 67 milliseconds. The shape of the power plot as a function of time is generally gaussian. The bottom plot shows a meteor echo that spills over into several range (height) bins. This echo began in a range bin of 98 km and as time progressed moved down into the adjacent height bins. The general shape of the power curve is still gaussian with time.

In routine operation of a ST/MST radar, a meteor echo appears; superimposed on the background echoes due to turbulent scattering. Consequently, depending on the length of the coherent averaging interval, a meteor echo can be lost in the background power level due to its short duration. Longer enduring meteor echoes can be selected from the combined data records which include meteor and turbulent echo returns using a post processing algorithm based on spatial and temporal properties of meteor echoes. This was done by AVERY et al., (1983) using the Poker Flat, Alaska MST radar. Based on their selection criterion, meteor echo rates were determined. Figure 3 shows a plot of the meteor echo count and the turbulent echo count as a function of height for three months at Poker Flat. Below 75 km, the meteor echo rate is almost constant with height. If the echoes selected by the algorithm were mostly noise and/or strong bursts of turbulent echoes, then we would expect, by symmetry, a double-peaked meteor distribution, corresponding to both the topside and bottomside of the turbulent echo region. Since the meteor echo profile shows only one peak, we conclude that the algorithm does indeed select, in the majority, true meteor echoes rather than noise spikes or intermittent turbulent echoes.

The profiles of meteor echo rates are. in comparison with the turbulent scatter profiles, much less variable. as seen in Figure 4. The meteor echo profile exhibits a stable, well-defined peak at about 92 km. The location and width of this peak is independent of the behavior of the turbulent scatter profile except during the summer months. During these months, near-continuous presence (80%) of strong turbulent echoes at Poker Flat masks virtually all the meteor echoes present. This is evident by the notch between 70-90 km in the echo height distribution during July. The echo rate corresponding to the peak in the echo height profile varies from about 2.2 echoes/hour in the summer to about 3.8 echoes/hour in the spring. The height of the peak is a minimum in the winter, while gradually rising in the spring and dropping in the fall.

The echo rate is clearly a function of power and antenna size as shown in Figure 5. This figure is a plot of the echo rate for the month of October over several years. During the first year, only one fourth of the antenna was in use and the power was 400 kw. In 1983 the power was brought up to maximum (3.2 Mw) and the full antenna was used. Still the echo rate is low compared to a normal meteor radar because in part, the echoes are not being selected in real time.

In our experiment at Jicamarca, we collected meteor echo return data in real time. This was done using computer software only. The detection and data collection algorithm uses a thresholding criterion for determining

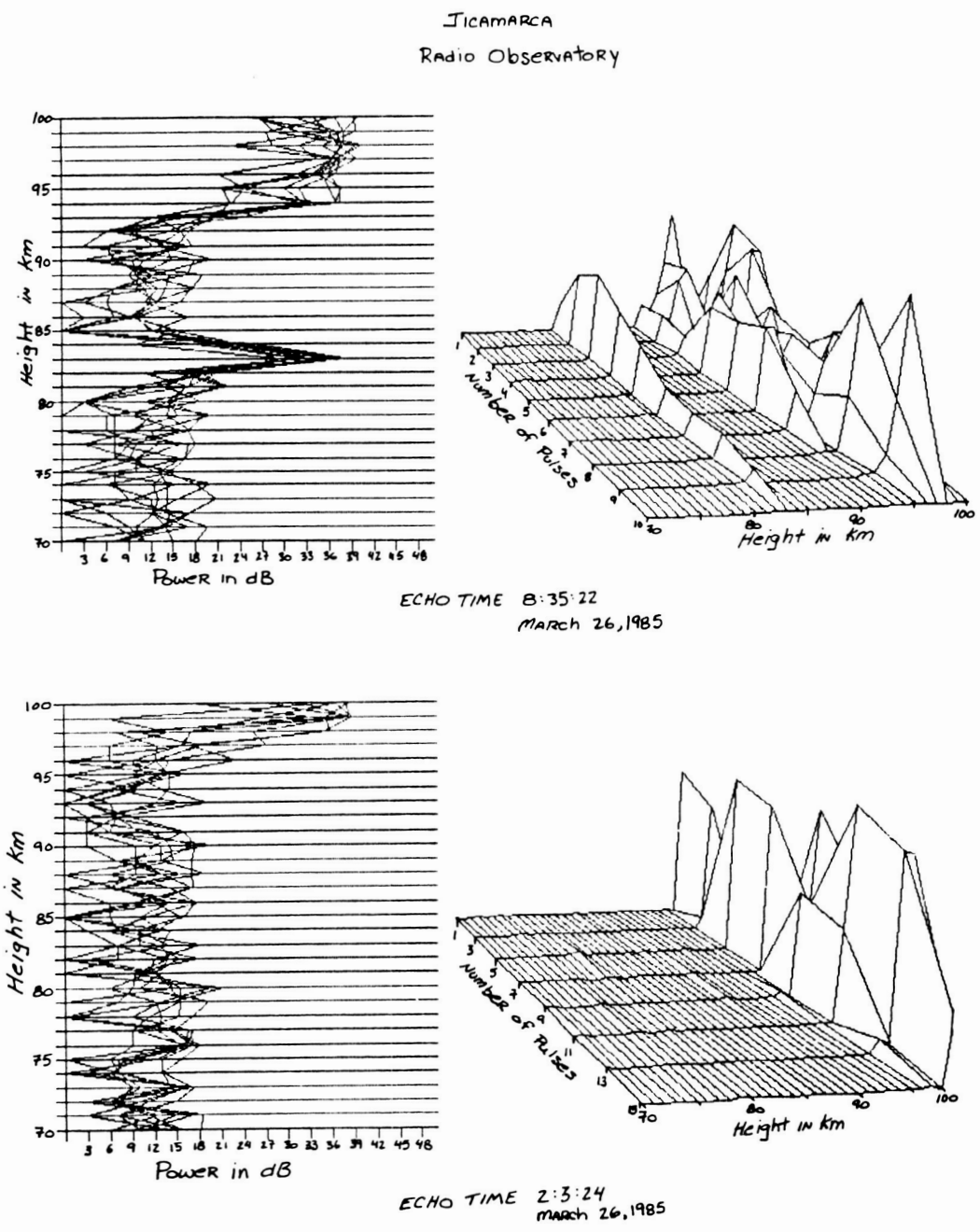

Fig. 2 Example of meteor echo returns from Jicamarca Radio Observatory, Peru.

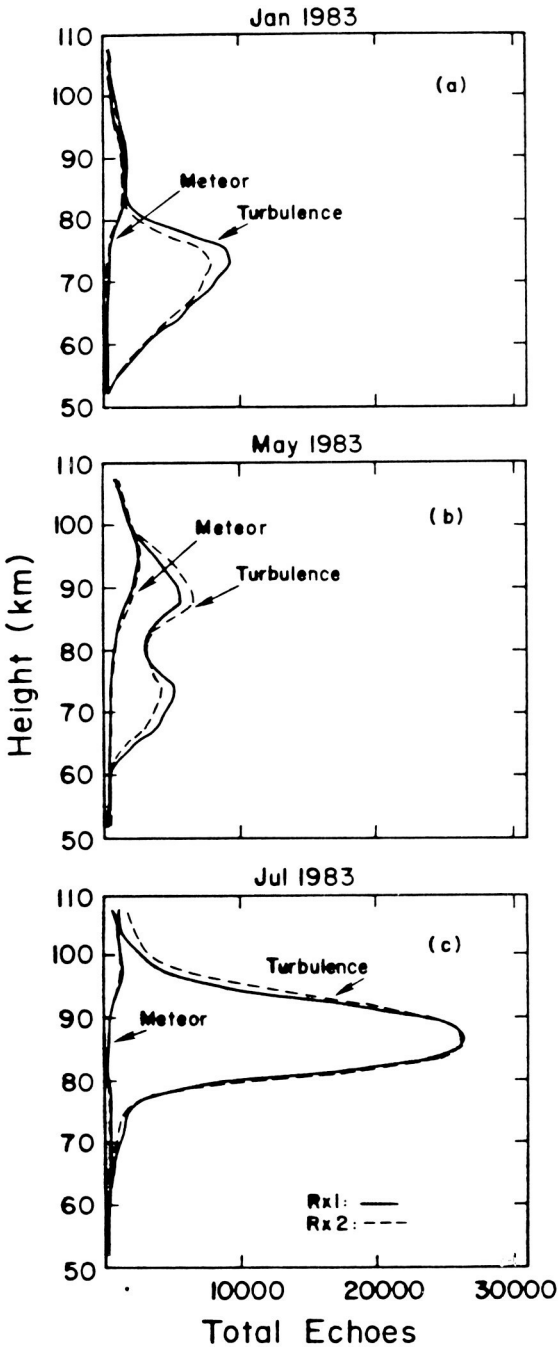

Fig. 3 Histograms of meteor echo and turbulence echo counts as a function of height at Poker Flat. Echoes determined from post processing criterion (from TETENBAUM and AVERY, 1986).

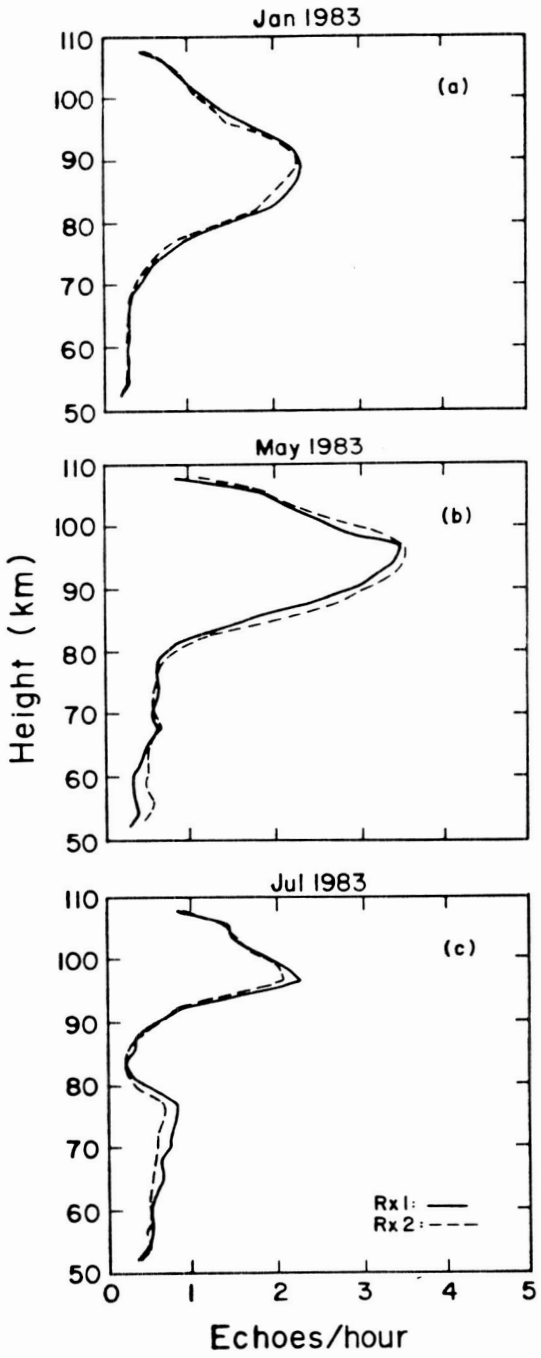

Fig. 4 Meteor echo rate as a function of height at Poker Flat. Echoes determined from post processing criterion (from TETENBAUM and AVERY, 1986).

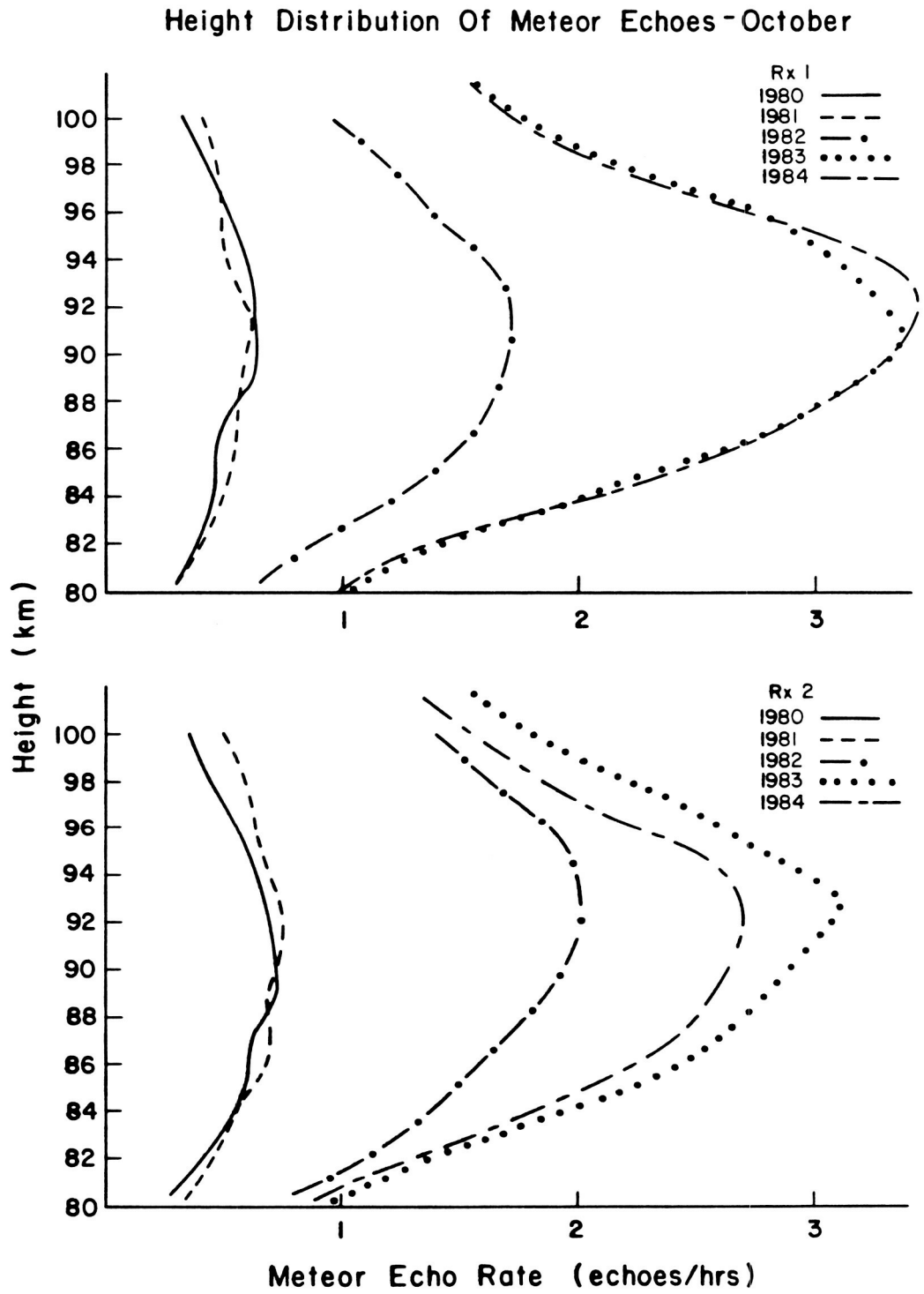

Fig. 5 Height distribution of meteor echoes in October for several different years (from TETENBAUM and AVERY, 1986).

the existence of a meteor echo. The threshold level, selected by the experimentor, is a fixed amount of dB above the background power level.

For the Jicamaraca experiment the threshold value was 9 dB. The background power level is determined at each range bin by a running average of the backscattered power from the previous 32 pulses. This is updated every pulse. Once a meteor echo is detected in a certain range bin, it must persist for at least 4 pulses (27 msec) but for no longer than 213 pulses (1.4 sec). In addition, the range bins on either side of the meteor echo range bin are checked. If the main echo power goes below the threshold value but appears in an adjacent range bin with a power level above the threshold value, we continue to take data in the new range bin. If this criterion is met, then the quadrature signals, range bin, and time of echo occurrence are recorded. Due to computer memory limitations, only the raw data was collected. We were unable to determine velocities in real time. Obviously this is less than ideal if there are a large number of echoes. Real time velocities could be calculated if a small personal computer was available and could be dedicated to the task of calculating Doppler frequencies.

A histogram of meteor echo count versus height is shown in Figure 6. The height profile peaks at higher altitudes than at Urbana, Illinois or Poker Flat, Alaska. This could be due to the equatorial location and position of the antenna beam, which was approximately 4 degrees off vertical. The equatorial atmosphere is more dense than the higher latitude atmosphere. Hence, meteors will ablate at higher altitudes. In addition, our thresholding algorithm may be preferentially deleting meteor trails that reach lower altitudes due to the length of the echo coming from that trail. More work needs to be done on refining the software algorithm. The temporal variation of echo count peaks in the early morning hours as expected.

The average echo duration as a function of height and time is also shown in Figure 6. In general, the echo duration, measured in number of radar pulses, is constant with time and height. We would expect this result given the random distribution of densities of sporadic meteors.

An alternative meteor detection scheme is being worked on at the University of Colorado. This scheme uses new technologies in hardware to incorporate the same detection ideas used in the software technique described above. The meteor echo detection and collection (MEDAC) system can be attached to many ST/MST radars and will operate in parallel with the normal data collection of turbulent echoes. A basic block diagram of the system is shown in Figure 7 (WANG, 1985).

Data is directly obtained from the radar receiver outputs and routed to the meteor system's own analog to digital converters. The system is completely independent of the ST/MST data acquisition system. The meteor selection criterion is now implemented in real-time rather than separating data after collection. The system is a two processor system. A foreground processor is dedicated to the task of echo detection. The processor performs dynamic thresholding on incoming echoes as they enter the system. A meteor will be detected if incoming echoes are above a certain threshold value. Threshold vales are dynamically maintained and updated for every signal. The Texas Instrument's TMS32010 microprocessor is the thresholding processor. The FIFO Data Collection subsystem shown in the diagram performs data collection of a meteor when one is present. The main components of the FIFO data collection subsystem are the MK4501 512 by

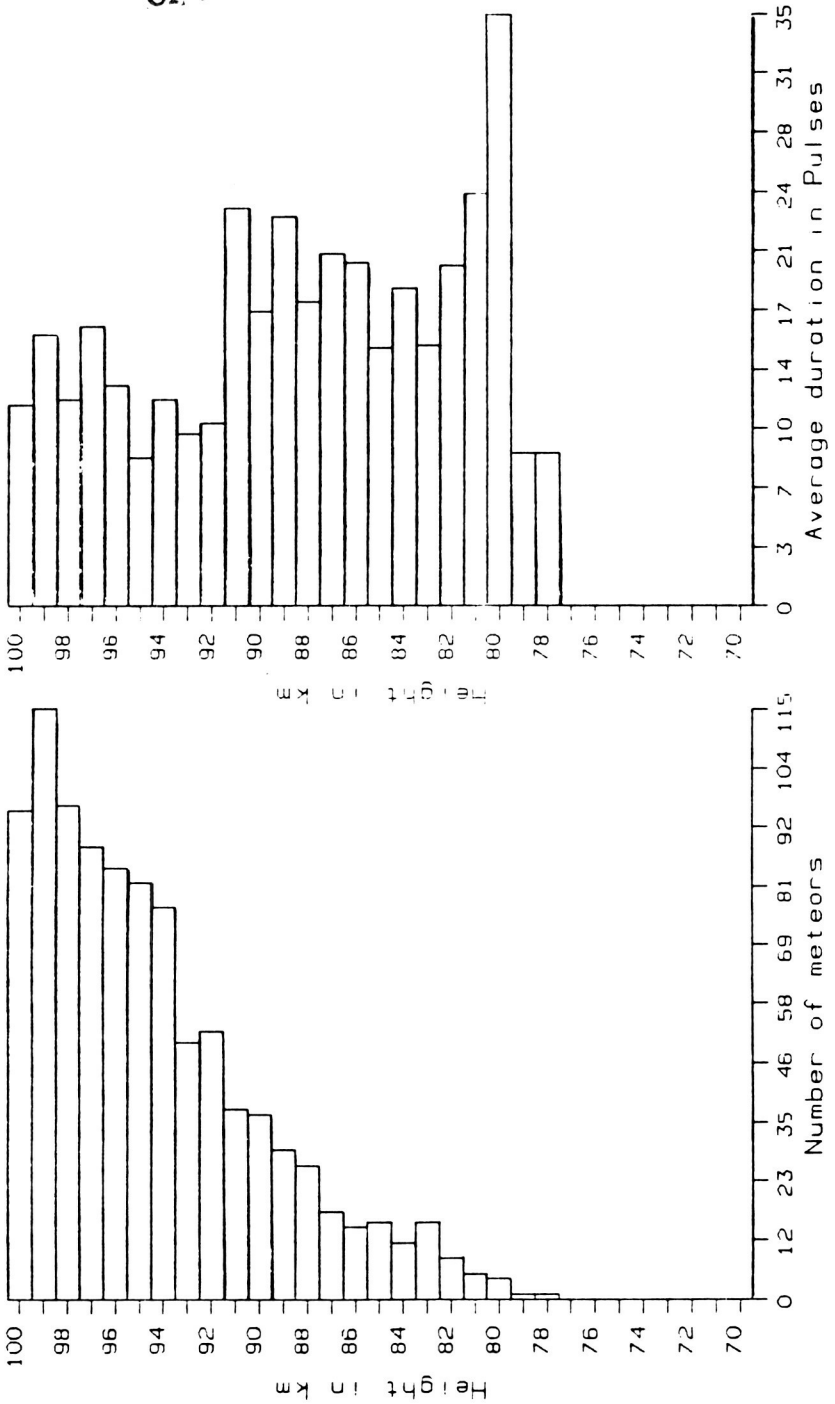

Fig. 6 Histograms of meteor echo count versus height and average echo duration versus height from Jicamarca.

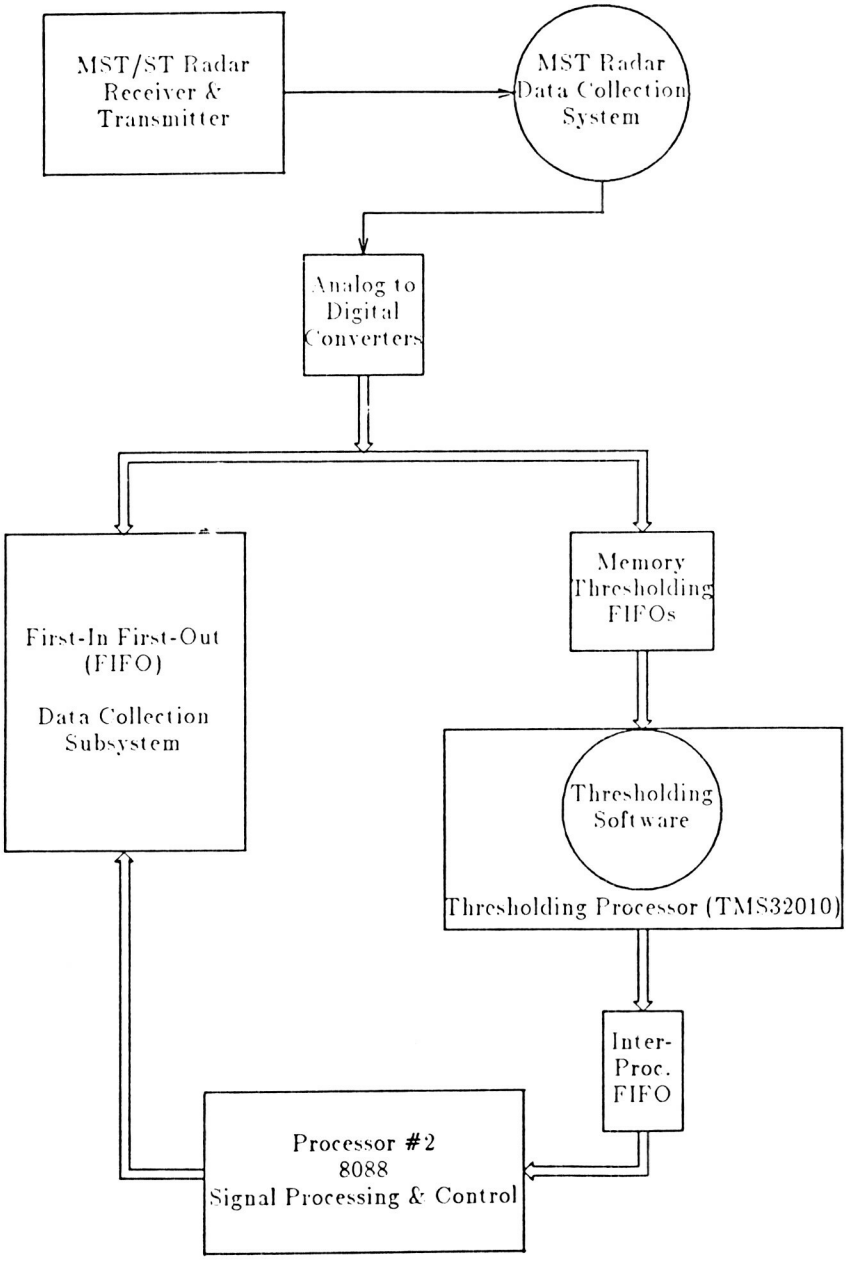

Fig. 7 Block diagram of MEDAC-system.

9-bit parallel input, output, first-in-first-out (FIFO) memory chips. Once a meteor has been found, the range bin and receiver number of the meteor is sent to the second processor through a shared memory between the processors. During operation the second processor is used for signal processing and data analysis of incoming meteors, as well as FIFO management.

A sample of winds determined from the Poker Flat post processing selection scheme is shown in Figure 8. The plot shows the winds determined from meteor echo returns with those determined from turbulent echoes. Clearly the agreement is good. Figure 9 shows a typical least squares sinusoidal fit to the wind determined from meteor echoes. The fit was done to a time series of 30 days of data of overlaying hourly wind averages from the 30 days into a single 24 hour period. Similar fits were done over shorter data sets with equally good results. From this type of data analysis, the tidal amplitude and phase structure can be calculated. Examples of the seasonal structures of the meridional semidiurnal tide from Poker Flat are shown in Figure 10. Because of the extensive data base provided by the Poker Flat, Alaska radar, seasonal changes in the winds and tides can be examined. Also shorter time scale variabilities can be assessed. Figure 11 shows the monthly mean wind climatologies which were determined from the Poker Flat MST meteor echoes.

Meteor echoes can be detected on ST/MST radars. If the radar is powerful (1 MW), enough meteor echoes can be selected from the turbulent echoes generally observed by the radar, to determine the winds and tides over monthly time scales. Using the less powerful ST radars, software or hardware detection schemes can be implemented to determine the mesospheric winds. The potential advantage of using meteor echo returns from ST radars is that it provides a relatively inexpensive way to obtain a measure of upper atmosphere winds. With the implementation of a network of these radars, we would have a significant number of upper atmosphere wind measurement stations. The cost for implementing the software algorithm would basically be the cost of a small computer. Two personal computers would be required to collect and analyze the meteor data for winds in real time. The hardware configuration we are developing will cost approximately $6,000. This is small compared to the $150,000 cost estimate for a ST radar.

REFERENCES

1. Avery, S. K., A. R., Riddle, B. B. Balsley, 1983: The Poker Flat, Alaska, MST Radar as a Meteor Radar, Radio Sci, 18, pp. 1021-1027.

2. Strauch, R. G., R. A. Kropfli, W. B. Sweezy, W. R. Moniger, and R. W. Lee, 1978: Improved Doppler Velocity Estimates by the Poly-Pulse-Pair Method, Proceeding of 18th Conf. on Radar Meteorology.

3. Tetenbaum, D. and S. K. Avery, 1986: Observations of Mean Winds and Tides in the Upper Mesosphere During 1980-1984 Using the Poker Flat, Alaska, MST Radar as a Meteor Radar, Submitted to J. Geophys. Res.

4. Wang, S. T.-H., 1985: The Design of a Microprocessor-Based System for Meteor Echo Detection and Collection on a MST Radar, M.S. Thesis, Dept. of Electrical and Computer Engineering, U. of Colorado, Boulder.

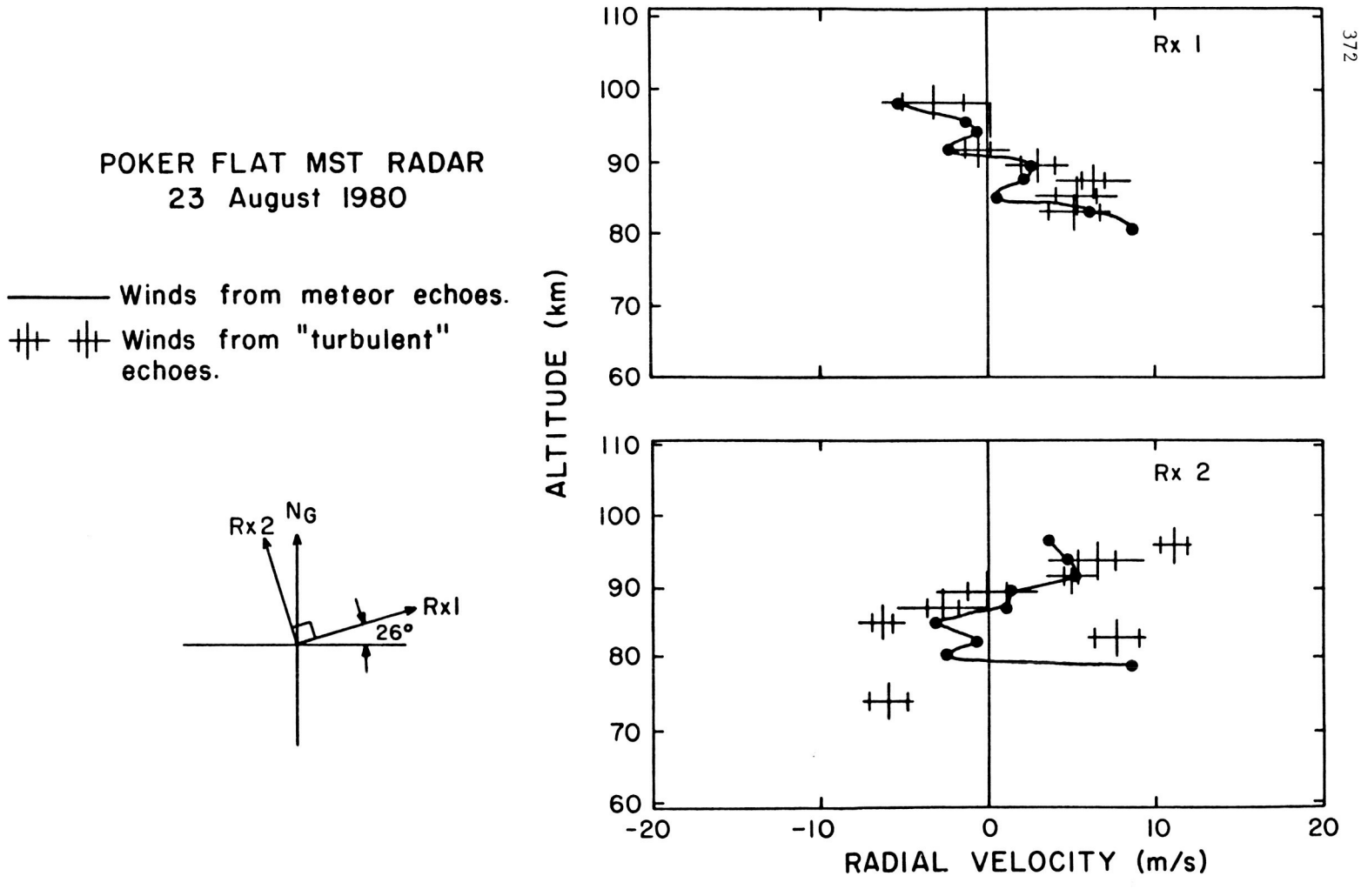

Fig. 8 Comparison of winds determined from meteor echoes with those obtained from turbulent echoes (from AVERY et al., 1983).

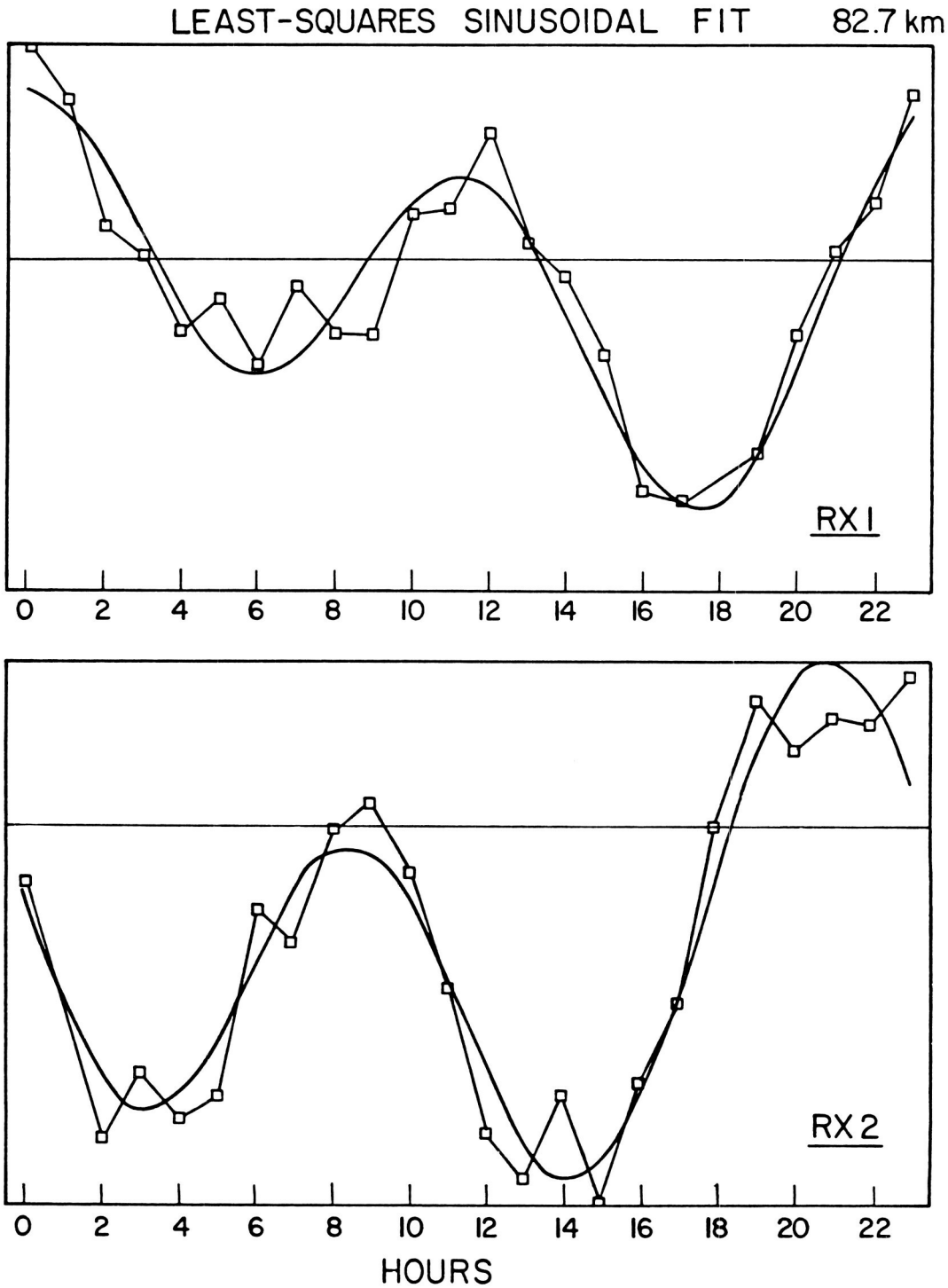

Fig. 9 Examples of least squares sinusoidal fits to Poker Flat data.

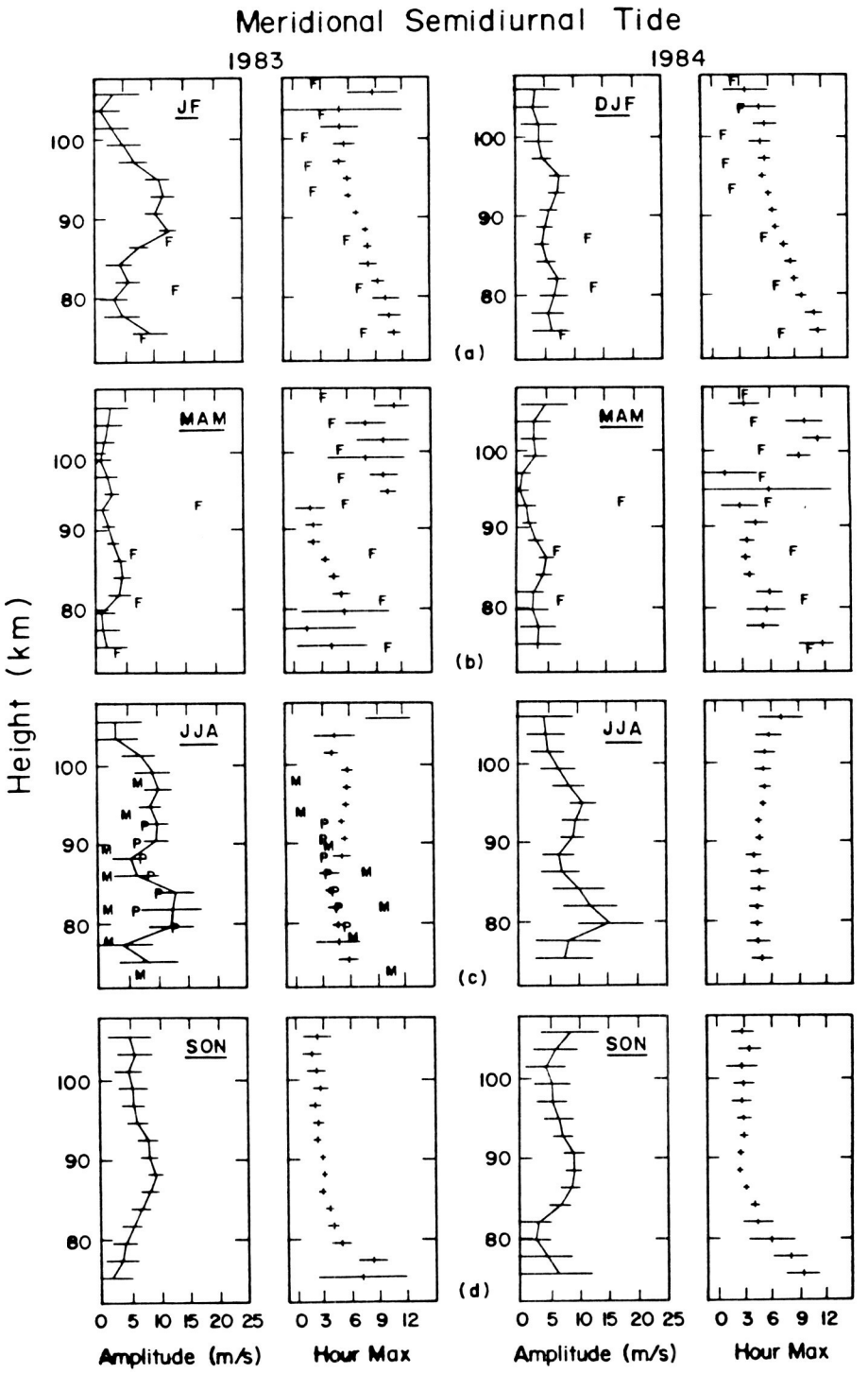

Fig. 10 Seasonal structures of the Poker Flat meridional semidiurnal tide (from TETENBAUM and AVERY, 1986).

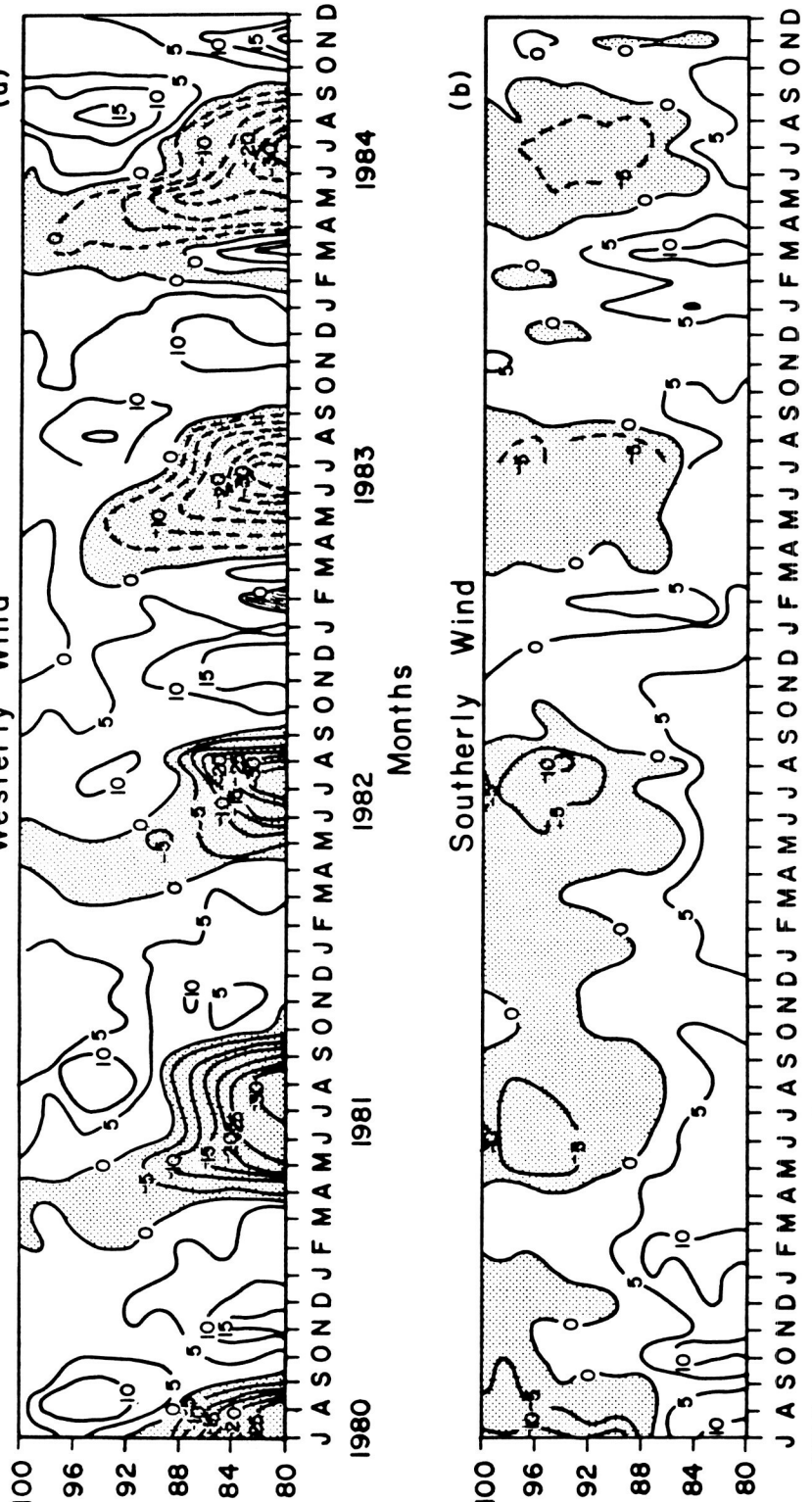

Fig. 11 Monthly mean wind climatologies at Poker Flat (from TETENBAUM and AVERY, 1986).